NEW INSIGHTS ON THE STRUCTURE AND MORPHOGENESIS OF BERNE VIRUS

Ana Garzón, Ana M. Maestre, Jaime Pignatelli, M. Teresa Rejas, and Dolores Rodríguez*

1. INTRODUCTION

Berne virus (BEV) is the protopype member of the torovirus genus and the only torovirus that can be grown in tissue culture. Torovirus genome consists of 6 ORFs, ORFs 1a and 1b, comprising the 5'-most two-thirds of the genome, and four additional ORFs encoding the structural proteins S, M, N, and HE. In BEV, ORF4, corresponding to the HE protein, is partially deleted, leaving only an 0.5-Kb fragment, that represents about one-third of the gene found in the bovine and porcine isolates. A distinct characteristic of the torovirus particles is the high morphological variability that they exhibit once they are released from infected cells. Spherical, oval, elongated, and kidney-shaped virions can be observed in the supernatant from infected cells after negative staining. The process of torovirus morphogenesis is still poorly understood and further studies are required to characterize this process at both morphological and molecular levels as well as to understand the structure of torovirus particles. All the information about the structure and morphogenesis of toroviruses comes from early studies performed by conventional electron microscopy examination of thin sections from cultured equine dermis cells infected with BEV,[1,2] as well as from intestinal tissue from calves infected with the bovine torovirus BRV.[3] These studies provided detailed descriptions of the different viral assemblies. However, in the past two decades new methods for structural analysis by electron microscopy have been developed to achieve an optimal preservation of the ultrastructure of cellular and viral components. Freeze-substitution is one of these high preservation methods that has been shown to greatly reduce artifactual changes in shape and size that can occur during fixation and dehydration of the sample when conventional treatments are used. Thus, in this work, BEV infected cells were fixed and treated by this technique to examine torovirus particles in the context of infected cells. To perform a thorough study of torovirus morphogenesis and to analyze virion structure, we need to identify viral components. For this purpose we have produced antibodies

* Centro Nacional de Biotecnologia, CSIC, Madrid, Spain

specific against BEV structural proteins. These antibodies were used to perform immunolabeling to detect viral proteins at the electron microscopy level and by immunofluorescence and confocal microscopy.

2. RESULTS AND DISCUSSION

2.1. Ultrastructure of Purified Virions

Viral particles released to the culture medium by BEV-infected Equine dermis (Ederm) cells were concentrated by centrifugation over a 20% sucrose cushion at 25000 rpm for 2 h. The pellet was resuspended in TEN buffer (10 mM Tris-HCl, pH 7.4, 1 mM EDTA, 150 mM NaCl) and layered over a 15–45% sucrose gradient that was centrifuged at 25000 rpm for 2 h. The fraction containing the virions was concentrated by ultracentrifugation. The characteristic polymorphism of torovirus particles was observed after negative staining of the purified preparation, and spherical, oval, elongated, kidney-shaped particles could be seen (Figure 1A, B). At higher magnification, surface projections or peplomers could be observed with more detail (Figure 1C, D).

2.2. Immunolabeling of Purified Virions

We have produced polyclonal antibodies against BEV-N protein by immunizing animals (mice, rats, and rabbits) with the protein produced as a recombinant product in the baculovirus expression system. We have also produced antibodies against the N and C termini of the M protein by immunizing animals with two synthetic peptides encompassing aminoacid residues 2 to 13 and 222 to 233, respectively. Specific reactivity of anti-N and anti-M antibodies was confirmed by Western blot using purified viral particles as antigen. In addition, monoclonal antibodies (mAb), G11 and AF3, were produced after immunization of mice with purified BEV virions. While the G11 mAb reacted in Western blot with the S protein, no reactivity against any viral protein was observed by this assay with the mAb AF3 (not shown).

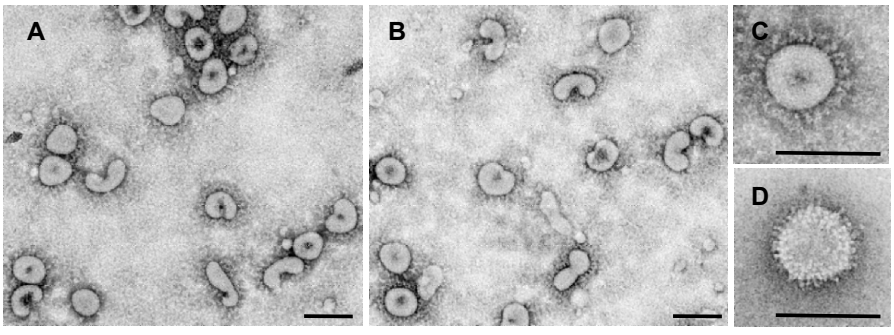

Figure 1. Polymorphism of BEV particles. Purified BEV virions adsorbed to collodion-carbon coated copper grids were negative stained for 1 min with 2% phosphotungstic acid (PTA) and examined by electron microscopy. (A) and (B) Low magnification fields showing particles with different shapes. (C) and (D) Isolated particles where surface peplomers can be clearly observed. Bars, 200 nm.

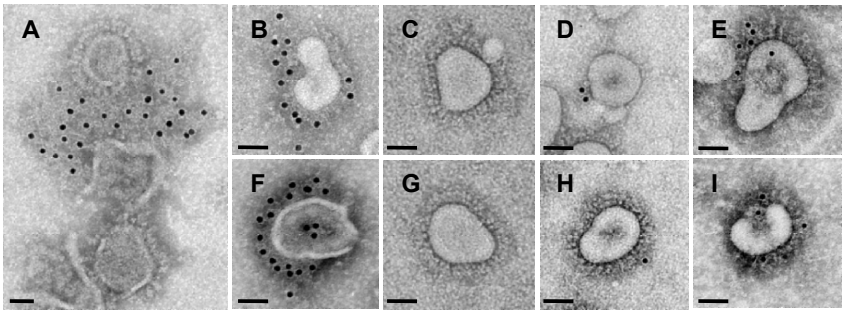

Figure 2. Immunolabeling of BEV particles. Purified BEV particles were incubated with different anti-BEV antibodies, followed by 10 nm gold-conjugated secondary antibodies and visualized by electron microscopy after negative staining with 2% PTA. (A) Anti-N polyclonal antibodies label the material released from virions partially disrupted by treatment at 4ºC with 0.05% Tween 20 in 100 mM Tris-HCl-10 mM $MgCl_2$, pH 8.0. (B) and (F) Particles labeled with a polyclonal serum against the N terminus of the M protein. (C) and (G) Antibodies to the C-terminus of the M protein do not label the surface of viral particles. (D) and (H) Weak but specific labeling with anti-S mAb G11. (E) and (I) Surface labeling with mAb AF3. Bars, 200 nm.

To further characterize these antibodies, immunolabeling of purified viral particles was performed using gold-conjugated secondary immunoglobulins, and viral particles were visualized after negative staining with 2% PTA. As shown in Figure 2A, anti-N antibodies label the internal material being released from viral particles after mild detergent treatment, but there is no reactivity with intact virions (not shown). Antibodies to the N terminus of the M protein clearly decorated the surface of the virion (Fig. 2B, F), while those directed against the C-terminal end of the protein do not react with intact particles (Fig. 2C, G). This result is in agreement with the topological model proposed for this protein by Den Boon et al.[4] Using *in vitro* protein synthesis and protease treatment they proposed that the N-terminus of the M protein would be exposed on the surface of the virion while the C-terminus would be buried inside the particle, in contact with the nucleocapsid. The mAbs G11 and AF3 provide a weak but specific surface labeling, and both are able to neutralize viral infectivity (not shown).

2.3. Analysis of the Ultrastructure of BEV-Infected Cells After Freeze-Substitution

Because it has been shown that freeze-substitution after ultrarapid freezing significantly improves preservation of biological samples as compared with conventional embedding methods,[5, 6] we used this methodology to study BEV-infected cells. Ederm cells were infected with BEV at high multiplicity of infection, fixed at 10 and 24 hpi and treated for freeze-substitution as previously described.[7] As observed in Figure 3, the milder dehydration conditions used in this procedure prevent extraction of cellular components and structure collapse. In the cytoplasm of these infected cells, we observed rod-like viral particles of homogenous size (Fig. 3A, B), and in some of them the profile of the viral envelope can be clearly distinguished (Fig. 3B). Secretory vesicles containing few viral particles can be seen at 10 hpi (Fig. 3C), and they become enlarged by 24 hpi (Fig. 3D). Tubular structures of similar diameter to viral particles but of variable length and devoid of membrane can be observed in the cytoplasm enclosed within rough-endoplasmic reticulum cisternae (Fig. 3E), but also in the nucleus (not shown). Most

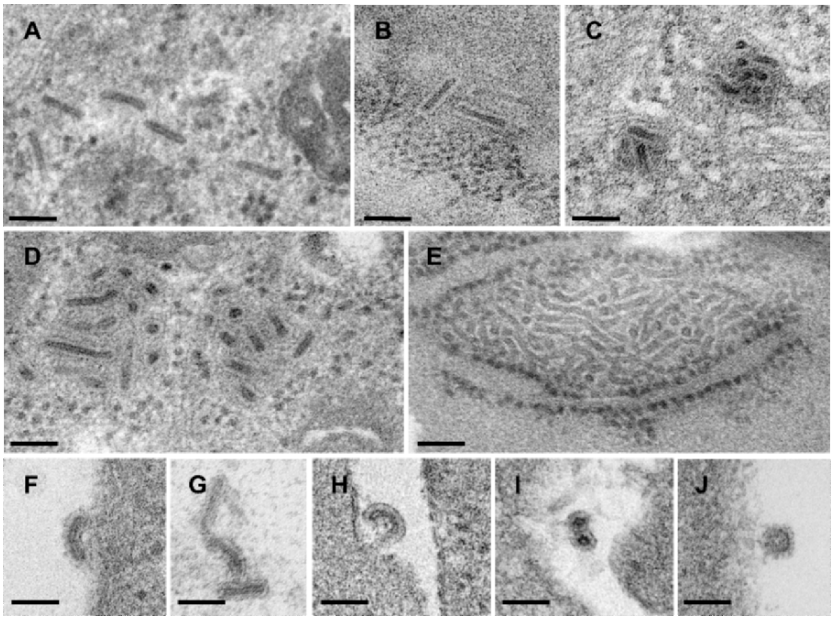

Figure 3. Thin sections of BEV-infected cells treated by freeze-substitution. Ederm cells infected with BEV at high multiplicity of infection were fixed *in situ* at 10 (A–C) or 24 hpi (D–J) with a mixture of 2% glutaraldehyde and 1% tannic acid in 0.4 M HEPES buffer (pH 7.5) for 1 h at RT. After washings, fixed cells were treated for freeze-substitution and embedding in epoxi-resin EML-812 as described in detail previously.[7] Ultrathin sections of the samples were stained with saturated uranyl acetate and lead citrate. (A) and (B) Rod-shaped particles of homogenous size. (C) and (D) Groups of particles enclosed within small (C) or large (D) secretory vesicles. (E) Tubular structures enclosed within a rough endoplasmic reticulum cisterna. (F)–(J) Extracellular viral particles, those in (F) and (G) show the same size and morphology as the intracellular rod-shaped particles seen in (A) and (B), although the profile of the viral envelope can be more clearly seen. In (H) and (I), elongated particles that are bent are observed in longitudinal (F) or cross - section (G). (J) Shows an example of a spherical particle surrounded by peplomers that are occasionally observed. Bars, 200 nm.

extracellular particles resemble the rod-shape particles seen in the cytoplasm (Fig. 3F, G), although some of them appear to be bent (longitudinally sectioned in Fig. 3H and cross-sectioned in Fig. 3I). Round particles with spikes on their surface can be occasionally seen (Fig. 3J). Our results are in agreement with those reported in previous studies,[1, 2, 3] and indicate that torovirus particles are elongated, with a rod-like appearance, resembling the morphology of the more recently described yellow head virus (YHV)[8] and gill associated virus (GAV),[9] both belonging to the *Roniviridae* family of the *Nidovirales* order. The different shapes adopted by torovirus particles outside the cells might be due to absence of a rigid structure that would impose a defined morphology.

2.4. Subcellular Localization of BEV Structural Proteins

We have examined the subcellular distribution of BEV proteins during the course of infection by confocal microscopy. At early times postinfection (6 h), the N protein is

mainly localized in the perinuclear area (Fig. 4A), while at later times it is widely distributed all over the cytoplasm (Fig. 4F, K). Similarly, at 6 hpi the two anti-M antibodies, against C (Fig. 4B) and N (Fig. 4C) termini, show a perinuclear localization of the protein, and this distribution is maintained with both antibodies up to 12 hpi (Fig. 4G, H), however, the signal almost disappears at later times with the antibody to the C terminus (Fig. 4L), while the anti-N terminus labels the cell surface at this time post-infection (Fig. 4M). This result indicates that once the protein is incorporated in the virion the C terminus would be inaccessible to the antibodies while the N terminus remains exposed on the surface of the virion, and this is also in agreement with the topological model previously proposed for the M protein.[4] The anti-S mAbG11 shows a diffuse distribution of the protein throughout the cytoplasm at the different times post-infection (Fig. 4D, I, N), while the signal associated to mAb AF3 can be first observed at 10–12 hpi in the perinuclear area (compare Fig. 4E and 4J), and at later times the signal is localized in the cell surface (Fig. 4O).

The perinuclear signal observed with the anti-M antibodies and with mAb AF3 is reminiscent of the signal observed with the protein marker of the endoplasmic reticulum–Golgi intermediate compartment ERGIC-53, and thus we performed a double labeling with the anti-M-N terminal antibody and a mAb specific for ERGIC-53 in BEV-infected cells. The result shown in Figure 5 reveals a clear co-localization of the two proteins, indicating that M is incorporated in this membranous compartment, and suggesting that, as occurs in coronaviruses, budding of progeny viruses occurs in this membranous compartment.

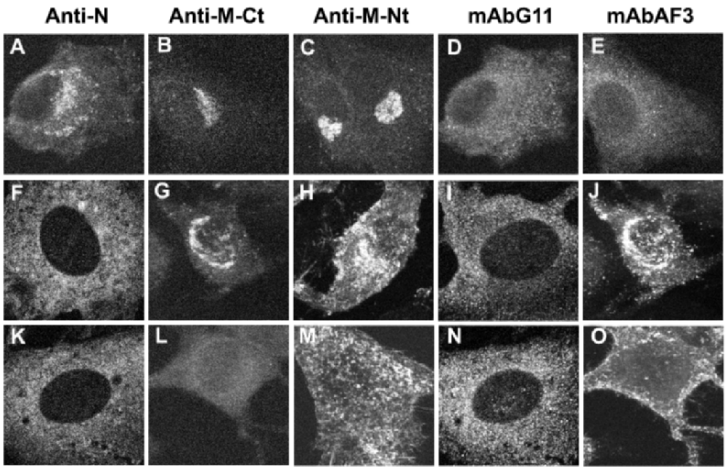

Figure 4. Intracellular distribution of BEV structural proteins. Ederm cells grown in coverslips were infected with BEV at high multiplicity and were fixed at 6 (A–E), 10 (F–J), and 16 (K–O) hpi. After fixing with 4% paraformaldehyde, cells were permeabilized in 0.1% Triton X100 and incubated with antibodies against the N protein (A–K), and against the C (B–L) and N (C–M) termini of M, and with the mAbs G11 (anti-S) and AF3 as indicated on the top of the figure, and cells were observed in a Bio-Rad Radiance 2000 confocal laser microscope.

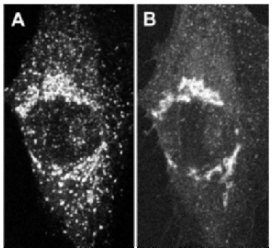

Figure 5. Co-localization of M protein with ERGIG-53. Ederm cells grown in coverslips were infected with BEV at high multiplicity. They were then fixed at 10 hpi. as described in legend to Figure 4, and simultaneously incubated with a mAb against ERGIC-53 (A) and a polyclonal serum against the N terminus of M protein (B).

3. ACKNOWLEDGMENTS

We are grateful to Raoul de Groot (University of Utrecht) for kindly providing BEV. We also thank Hans Peter Hauri (Biozentrum, University of Basel) for his anti-ERGIC-53 antibody, Sylvia Gutiérrez for her support with the confocal microscope, Milagros Guerra and Francisca Ocaña for their excellent technical assistance on sample preparation for electron microscopy, and Leonor Kremer for sharing her expertise in preparing monoclonal antibodies.

This work was supported by a grant from the Ministerio de Educación y Ciencia of Spain (BIO-2002-03739).

4. REFERENCES

1. M. Weiss, F. Steck, and M. C. Horzinek, Purification and partial characterization of a new enveloped RNA virus (Berne Virus), *J. Gen. Virol.* **64**, 1849-1858 (1983).
2. M. Weiss and M. C. Horzinek, Morphogenesis of Berne Virus (Proposed Family Toroviridae), *J. Gen. Virol.* **67**, 1305-1314 (1986).
3. J. A. Flagerland, J. F. L. Pohlenz, and G. N. Woode, A morphological study of the replicaton of Breda Virus (Proposed Family Toroviridae), *J. Gen. Virol.* **67**, 1293-1304 (1986).
4. J. A. Den Boon, E. J. Snider, J. Krinjse-Locker, M. C. Horzinek, and P. J. M. Rottier, Another triple-spanning envelope protein among intracellular budding RNA viruses: the torovirus E protein, *Virology* **182**, 655-663 (1991).
5. D. M. R Harvey, Freeze-substitution, *J. Microsc.* **127**, 209-221 (1982).
6. S. Hippe-Sanwald, The impact of freeze-substitution on biological electron microscopy. *Microsc. Res. Tech.* **24**, 400-422 (1993).
7. C. Risco, J. R. Rodríguez, C. López-Iglesias, J. L. Carrascosa, M. Esteban, and D. Rodríguez, Endoplasmic reticulum-Golgi intermediate compartment membranes and vimentin filaments participate in vacccinia virus assembly, *J. Virol.* **76**, 1839-1855 (2002).
8. C. Chantanachookin, S. Boonyaratpalin, J. Kasornchandra, D. Sataporn, U. Ekpanithanpong, K. Supamataya, S. Riurairatana, and T. W. Flegel, Histology and ultrastructure reveal a new granulosis-like virus in Penaeus monodon affected by yellow-head disease, *Dis. Aquat. Organ.* **17**, 145-157 (1993).
9. J. A. Cowley, C. M. Dimmock, C. Wongteerasupaya, V. Boonsaeng, S. Panyim, and P. J. Walker, Yellow head virus from Thailand and gill-associated virus from Australia are closely related but distinct prawn viruses, *Dis. Aquat. Organ.* **36**, 153-157 (1999).